World Academy of Science, Engineering and Technology
International Journal of Civil and Environmental Engineering
Vol:7, No:2, 2013

Approximate Tension Buckling Capacity of Thin Edge-Cracked Web Plate Subjected to Pure Bending

Sebastian B. Mendes

***Abstract*—**The presence of a vertical edge-crack within a web plate subjected to pure bending induces local compressive stresses about the crack which may cause tension buckling. Approximate theoretical expressions were derived for the critical far-field tensile stress and bending moment capacity of an edge-cracked web plate associated with tension buckling. These expressions were validated with finite element analyses and used to investigate the possibility of tension buckling in web-cracked trial girders. It was found that tension buckling is an unlikely occurrence unless the web is relatively thin or the crack is very long.

***Keywords*—**Fatigue crack, tension buckling, Rayleigh-Ritz, structural stability.

Open Science Index, Civil and Environmental Engineering Vol:7, No:2, 2013 publications.waset.org/15693/pdf

I. Introduction

WEB plates form an integral part of beams and plate girders. These types of flexural members are oftentimes subjected to sub-critical cyclic bending stresses, as in the case of highway bridge plate girders. The fatigue loading produces fluctuating tensile stress concentrations at locations of discontinuity within a beam or plate girder, such as at imperfections in the welds connecting the web plate to the tension flange [1-11]. Over time, the fluctuating tensile stress concentrations may cause pre-existing microscopic flaws to form into through-thickness macrocracks [12, 13]. The fatigue loading may then cause a crack to propagate through the web plate in a direction transverse to the far-field tensile stresses [1-11]. One of the potential failure modes made possible by the presence of a growing crack is so-called tension buckling [14]. This phenomenon manifests itself in the form of wrinkling in the immediate region adjacent to the crack.

Relatively few studies have investigated the effects of cracks on the reduction in strength of beam-like structures [15, 16]. However, far more studies have examined the effects of holes and slots on the reduction in strength of beams and plate girders [17-21]. Although these studies did not consider tension buckling, other research has investigated tension buckling in cracked plates using experimental [22, 23], numerical [24-28], and theoretical methods [25, 26, 29].

The objective of this study was to develop a theoretical expression for the bending moment capacity, M_n, associated with tension buckling of a thin web plate containing a through-thickness fatigue edge-crack using various approximations. Results obtained from the expression were compared with results from finite element (FE) analyses using the general FE software ABAQUS. The bending moment capacities were then plotted as functions of edge-crack length for various web plate thicknesses and interesting conclusions were drawn.

The focus of this study was specific to a thin web plate that is part of an I-shaped beam or plate girder subjected to pure bending (see Fig. 1). The fatigue edge-crack of length *2a* was assumed to originate along the boundary between the web plate and the tension flange and extend vertically through the web. The tensile stress being applied to the base of the edge-crack was assumed to be equal to the far-field tensile stress, σ_o, at the extreme fiber of the web plate as obtained from beam theory. The web plate was assumed to be a rectangular, homogeneous, linear isotropic elastic, thin plate with clamped support conditions along the longitudinal edges bordering the flange plates (see Table I).

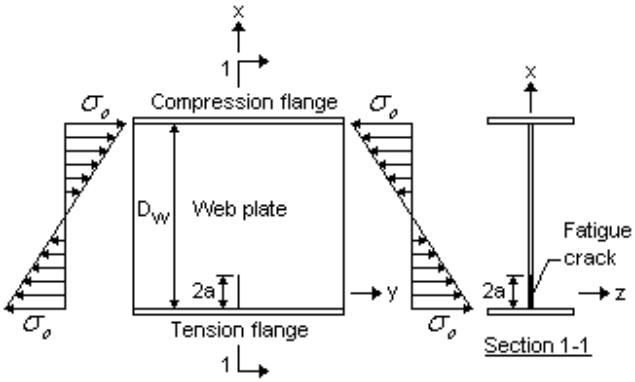


Fig. 1 I-shaped beam or plate girder under pure bending showing location of through-thickness fatigue edge-crack within web plate

TABLE I
Web Plate Geometric Boundary Conditions

Edge (x, y)	U_x	U_y	U_z	R_x	R_y	R_z
(-a, y)	x	0	x	x	x	x
(D_w - a, y)	x	0	x	x	x	x

II. Compressive Stress Distributions

The presence of the through-thickness edge-crack in the loaded web plate induces transverse compressive stresses, σ_x, adjacent to the crack which may cause local buckling (see Fig. 2). The exact compressive stress distribution is difficult to obtain due to the non-symmetric configuration and complicated boundary conditions of the crack. As an alternative, the transverse stress distribution is approximated by considering the edge-crack to be a central crack located

S.B. Mendes is a Doctoral candidate at the Department of Civil and Environmental Engineering, University of Rhode Island, Kingston, RI 02881 USA (phone: 203-815-7640; e-mail: mendessb@my.uri.edu).

within an infinite plate loaded by linearly varying far-field tensile stress distributions (see Fig. 3).

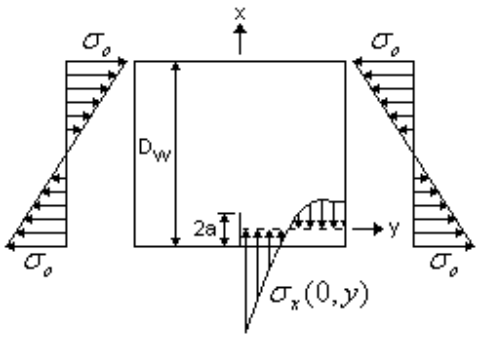


Fig. 2 Web plate showing distribution of transverse stresses along the positive y-axis adjacent to the edge-crack

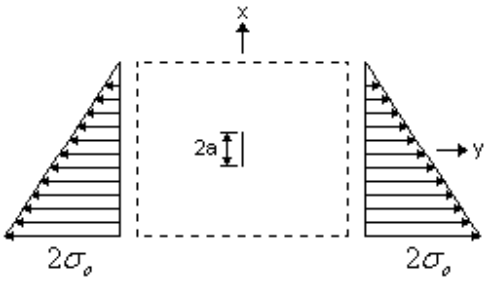


Fig. 3 Central crack within an infinite plate subjected to linearly varying far-field tensile stress distributions

The case in Fig. 3 is more general and the stress field about the central crack can be readily approximated by employing the principle of superposition [30, 31]. This stress field is obtained by superimposing the stress field for the case in Fig. 3 without a crack with the stress field for the case of a central crack within an infinite plate subjected to linearly varying crack face tensile stresses, $\sigma_y(x_o)$ (see Fig. 4a). These tensile stresses are described by the function.

$$\sigma_y(x_o) = \pm\sigma_o\left(\frac{2x_o}{D_w} + \frac{2a}{D_w} - 1\right) \tag{1}$$

where x_o is the distance along the x-axis measured from the origin of the coordinate system and D_w is the depth of the web plate. The variation of the crack face tensile stresses is identical to the stress variation of the case in Fig. 3. The maximum tensile stress occurs at $x_o = -a$ and is equal to σ_o.

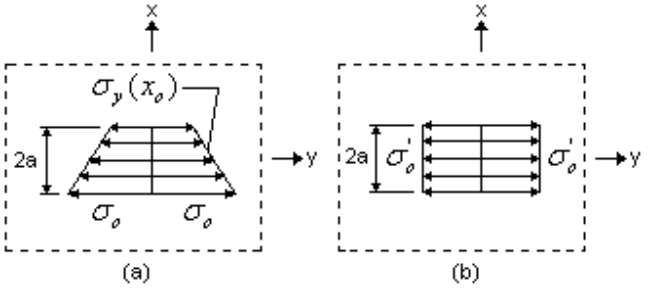


Fig. 4 Central crack within an infinite plate subjected to (a) linearly varying and (b) uniform crack face tensile stresses

The superimposed stress field of the case in Fig. 3 without a crack has no effect on the transverse stress distribution about the central crack, and so the stress field is sought for the case in Fig. 4a. This case is greatly simplified by recognizing from (1) that, for small crack lengths and large web plate depths, σ_o is nearly equal to the crack face tensile stresses at the crack end given by $\sigma_y(a)$. The distribution of crack face tensile stresses is therefore approximated as uniform tensile stress, σ_o' (see Fig. 4b).

The magnitude of σ_o' is taken as the average of σ_o and $\sigma_y(a)$ expressed by

$$\sigma_o' = \pm\sigma_o\left(\frac{2a}{D_w} - 1\right) \tag{2}$$

The two-dimensional stress field of the case in Fig. 4b is obtained by employing the Airy stress function, $F(x,y)$. The Airy stress function must satisfy any given boundary conditions and the biharmonic equation given by [31]

$$\nabla^4 F = \frac{\partial^4 F}{\partial x^4} + 2\frac{\partial^4 F}{\partial x^2 \partial y^2} + \frac{\partial^4 F}{\partial y^4} = 0 \tag{3}$$

which identically satisfies the equilibrium and compatibility equations. The stress field is expressed as [31]

$$\sigma_x = \frac{\partial^2 F}{\partial y^2} \qquad \sigma_y = \frac{\partial^2 F}{\partial x^2} \qquad \tau_{xy} = -\frac{\partial^2 F}{\partial x \partial y} \tag{4}$$

For elastic bodies containing cracks, the Airy stress function may be expressed in terms of the Westergaard stress function, $Z(\zeta)$, as [32]

$$F = \mathrm{Re}\,\overline{\overline{Z}} + y\,\mathrm{Im}\,\overline{Z} \tag{5}$$

where

$$Z' = \frac{dZ}{d\zeta} \qquad Z = \frac{d\overline{Z}}{d\zeta} \qquad \overline{Z} = \frac{d\overline{\overline{Z}}}{d\zeta} \tag{6}$$

Open Science Index, Civil and Environmental Engineering Vol:7, No:2, 2013 publications.waset.org/15693/pdf

Open Science Index, Civil and Environmental Engineering Vol:7, No:2, 2013 publications.waset.org/15693/pdf

and ζ is the complex variable $\zeta = x + iy$. Substitution of (5) into (4) results in the stress field becoming

$$\begin{aligned}\sigma_x &= \mathrm{Re}\, Z - y\,\mathrm{Im}\, Z' \\ \sigma_y &= \mathrm{Re}\, Z + y\,\mathrm{Im}\, Z' \\ \tau_{xy} &= -y\,\mathrm{Im}\, Z'\end{aligned} \tag{7}$$

The Westergaard stress function for the case in Fig. 4b is expressed as [33]

$$Z = \frac{\sigma_o'}{\pi\sqrt{\zeta^2 - a^2}} \int_{-a}^{a} \frac{\sqrt{a^2 - x_o^2}}{\zeta - x_o}\, dx_o \tag{8}$$

Evaluating the integral results in [34]

$$Z = \sigma_o' \left(\frac{\xi}{\sqrt{\xi^2 - a^2}} - 1 \right) \tag{9}$$

Substituting (2) and (9) into $(7)_1$ and setting $x = 0$ results in the following expression for the two-dimensional transverse stress distribution along the positive y-axis of the central crack shown in Fig. 3

$$\sigma_x(0, y) = \sigma_o \left(\frac{2a}{D_w} - 1 \right) \left[\frac{y^3}{\left(y^2 + a^2\right)^{\frac{3}{2}}} - \frac{2y}{\sqrt{y^2 + a^2}} + 1 \right] \tag{10}$$

Alternatively, setting $x = \pm a$ results in the transverse stress distribution at the crack ends given by

$$\begin{aligned}\sigma_x(\pm a, y) = -\sigma_o \left(\frac{2a}{D_w} - 1 \right) \Bigg\{ & \mathrm{Re} \left[\frac{a + iy}{\sqrt{(a + iy)^2 - a^2}} - 1 \right] \\ & - y\,\mathrm{Im} \left[\frac{1}{\sqrt{(a + iy)^2 - a^2}} - \frac{(a + iy)^2}{\left((a + iy)^2 - a^2\right)^{\frac{3}{2}}} \right] \Bigg\}\end{aligned} \tag{11}$$

Based on the prior assumption considering the edge-crack to be a central crack within an infinite plate, (10) approximately describes the transverse stress distribution at the middle of the crack on the positive y-axis, and (11) approximately describes the transverse stress distribution along the clamped edge of the web plate and at the far end of the crack (see Fig. 5).

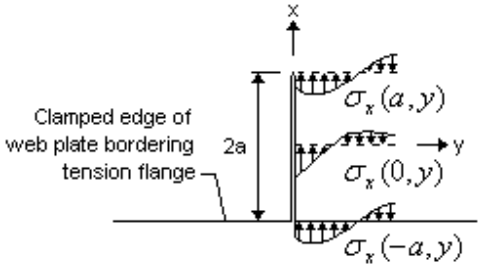


Fig. 5 Transverse stress distributions at the middle and ends of edge-crack

III. Tension Buckling Capacity

The transverse stress distributions given by (10) and (11) are used to calculate the local buckling stress of the portion of web plate adjacent to the edge-crack by employing the Rayleigh-Ritz method. This portion of plate is assumed to be a rectangular embedded plate (see Fig. 6a) with clamped support conditions along three edges and a free edge formed by the edge-crack (see Fig. 6b). This assumption is deemed to be reasonable in light of the first buckling mode shapes obtained by Brighenti [25] during FE analyses of centrally cracked plates in tension.

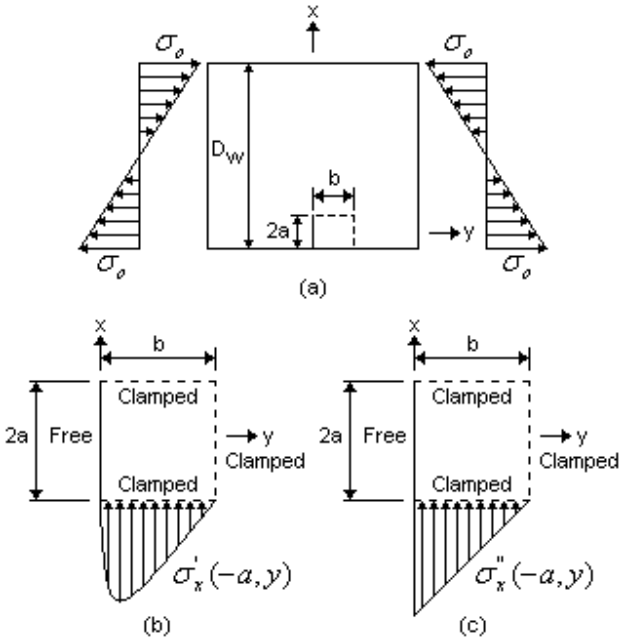


Fig. 6 (a) Location of embedded plate adjacent to edge-crack with (b) exact and (c) approximate transverse stress distributions

The compressive stress distribution adjacent to the crack is approximated by loading the clamped edge of the embedded plate bordering the tension flange with a transverse compressive stress distribution, $\sigma_x'(-a, y)$, taken as the average of (10) and (11), given by

$$\sigma_x'(-a, y) = \frac{\sigma_x(0, y) + \sigma_x(a, y)}{2} \tag{12}$$

Open Science Index, Civil and Environmental Engineering Vol:7, No:2, 2013 publications.waset.org/15693/pdf

Substituting (10) and (11) into (12) results in a lengthy expression for the transverse stress distribution (see Fig. 6b). Examination of (12) reveals that the stress distribution is triangular in shape and can be simplified as a linear distribution, $\sigma_x''(-a, y)$ (see Fig. 6c). The slope is taken as one half of (2) divided by the width, b, of the embedded plate, and the x-intercept is taken as one half of (2). The value of b is assumed to be equal to the extent of $\sigma_x'(-a, y)$ in compression and is determined by setting (12) equal to zero and solving for y resulting in

$$b \cong 1.16a \tag{13}$$

Accordingly, the simplified transverse stress distribution becomes

$$\sigma_x''(-a, y) = \frac{\sigma_o}{2}\left(\frac{2a}{D_w} - 1\right)\left(1 - \frac{y}{b}\right) \tag{14}$$

In accordance with the Rayleigh-Ritz method, the buckled shape of the embedded plate is assumed to take on a form described by a deflection function, $w(x,y)$. The deflection function satisfies the geometric boundary conditions indicated in Fig. 6b and includes an arbitrary variable, A. The change in total potential energy, Π, with respect to A is set to zero and the stress distribution given by (14) enabling this equilibrium is solved for. The total potential energy of the embedded plate is given by [35]

$$\begin{aligned}\Pi = \int_V W dV - \int_S T_i u_i dS = \frac{D}{2}\int_0^b \int_{-a}^{a} \left\{ \left(\frac{\partial^2 w}{\partial x^2} + \frac{\partial^2 w}{\partial y^2}\right)^2 \right. \\ \left. - 2(1-\upsilon)\left[\left(\frac{\partial^2 w}{\partial x^2}\right)\left(\frac{\partial^2 w}{\partial y^2}\right) - \left(\frac{\partial^2 w}{\partial x \partial y}\right)^2\right] \right\} dxdy \\ + \frac{1}{2}\int_0^b \int_{-a}^{a} \sigma_x''(-a, y)\left(\frac{\partial w}{\partial x}\right)^2 dxdy\end{aligned} \tag{15}$$

where W is the strain-energy density function, V is the volume of the plate, T_i are the applied surface tractions, u_i are the corresponding displacements, and S is the surface over which the tractions are applied. D is the plate rigidity given by

$$D = \frac{Et_w^3}{12(1-\nu^2)} \tag{16}$$

where E is the modulus of elasticity, ν is Poisson's ratio, and t_w is the web plate thickness.

The geometric boundary conditions indicated in Fig. 6b are explicitly expressed as

$$w(-a, y) = 0 \qquad w(a, y) = 0 \qquad w(\pm x, b) = 0$$

$$\frac{dw(-a, y)}{dx} = 0 \qquad \frac{dw(a, y)}{dx} = 0 \qquad \frac{dw(\pm x, b)}{dy} = 0 \tag{17}$$

A simple deflection function of the following form satisfies these conditions

$$w = A(y-b)^2 \cos^2\left(\frac{\pi x}{2a}\right) \tag{18}$$

Substituting (13), (14), and (18) into (15) results in an expanded expression for the total potential energy. Setting the change in total potential energy with respect to A to zero requires that

$$\frac{\delta \Pi}{\delta A} = 0 \tag{19}$$

From calculus of variations, $\delta(A^2) = 2A\,\delta A$, which allows for A to be canceled from the expanded expression [35]. Solving for the far-field tensile stress and dividing the result by t_w gives

$$\sigma_{cr} = 2.97\frac{Et_w^2 D_w (1.56 - \nu)}{a^2 (D_w - 2a)(1-\nu^2)} \le \sigma_Y \tag{20}$$

where σ_Y is the uniaxial yield strength of the web plate material. This expression represents an approximation of the critical far-field tensile stress at the extreme fiber of the web plate corresponding to local buckling of the portion of web adjacent to the edge-crack. It follows that the bending moment capacity of the web plate associated with tension buckling is given by

$$M_n = \sigma_{cr} S \tag{21}$$

where S is the elastic section modulus of the web plate with respect to the strong axis of bending.

IV. FE Analysis

FE analyses were employed to validate the critical far-field tensile stress given by (20). ABAQUS was used to model four full-scale trial plate girders with length, L, of 5 m in a cantilevered configuration as shown in Fig. 7a. An external bending moment, M_o, was applied to the free end of each girder such that a constant internal bending moment was induced throughout the entire length (see Fig. 7b). Each girder was modeled with a constant web plate depth of 127 cm and flange width, b_f, of 35 cm (see Fig. 7c).

A different web plate thickness was assigned to each trial girder. The flange thickness, t_f, was assumed to be twice the thickness of t_w. A vertical edge-crack was modeled at the mid-span of each girder on the tension side of the web plate. Four different crack lengths were tested for each trial girder for a total of 16 tests (see Table II). Also, each girder was modeled

with the typical material properties of alloy steel (modulus of elasticity, $E = 200\ GPa$; yield strength, $\sigma_Y = 345\ MPa$; Poisson's ratio, $v = 0.3$).

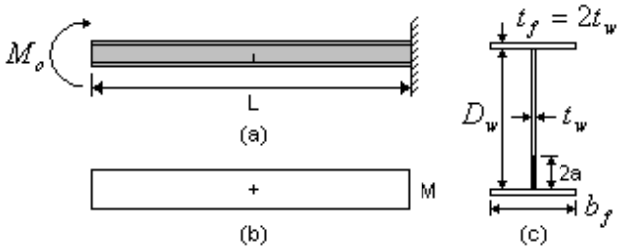


Fig. 7 (a) Cantilevered configuration of trial plate girders with (b) corresponding internal bending moment diagram and (c) section dimensions

TABLE II
TRIAL PLATE GIRDER GEOMETRIC PROPERTIES

Plate Girder (PG)	Web Thickness, t_w (cm)	Crack Length, 2a (cm)	Plate Girder (PG)	Web Thickness, t_w (cm)	Crack Length, 2a (cm)
PG-1a	0.15	4.0	PG-3a	0.60	4.0
PG-1b	0.15	8.0	PG-3b	0.60	8.0
PG-1c	0.15	16	PG-3c	0.60	16
PG-1d	0.15	32	PG-3d	0.60	32
PG-2a	0.30	4.0	PG-4a	1.20	4.0
PG-2b	0.30	8.0	PG-4b	1.20	8.0
PG-2c	0.30	16	PG-4c	1.20	16
PG-2d	0.30	32	PG-4d	1.20	32

PG-3 and PG-4 possessed realistic girder dimensions whereas the proportions of PG-1 and PG-2 were purely hypothetical for the purpose of demonstrating the tension buckling phenomenon. The trial girders were meshed with 10-node quadratic tetrahedron solid elements. Partitions were created around the crack to allow for a finer mesh in the vicinity of the crack. The crack itself was modeled as a thin extrusion through the web.

PG-1 through PG-4 were first used to validate the transverse compressive stress distribution at the middle of the crack given by (10). M_o was set such that the far-field tensile stress at the extreme fiber of the web was equal to 172.5 MPa. The transverse compressive stress distributions for each trial girder obtained using (10) and the FE analyses demonstrated a close correlation (see Fig. 8).

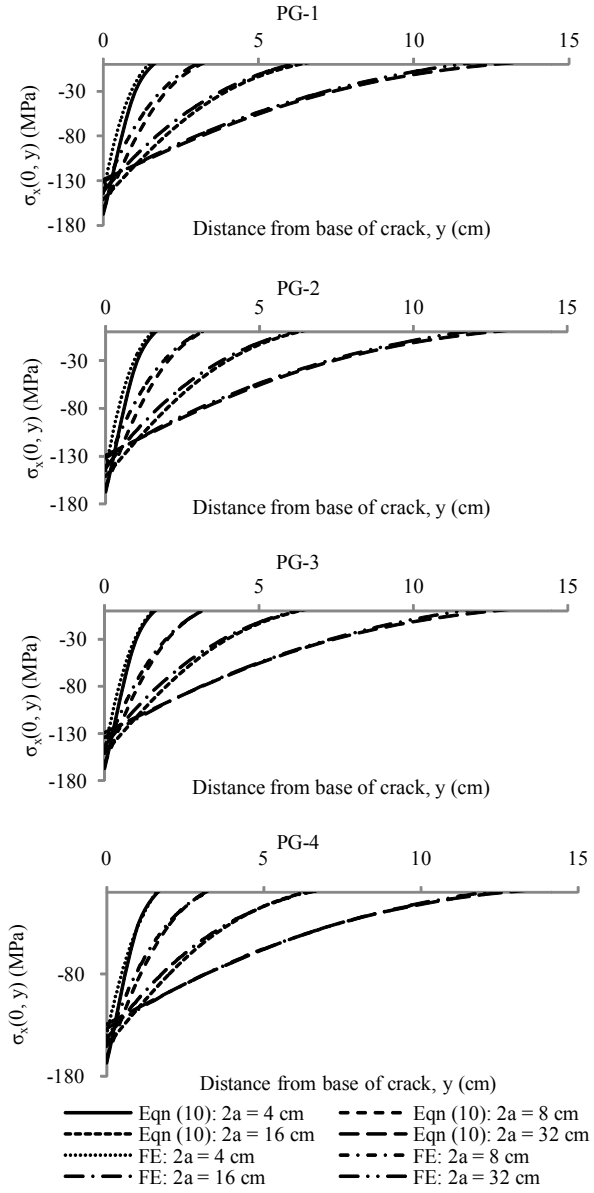


Fig. 8 Transverse compressive stress distributions at middle of crack obtained analytically and numerically for each trial girder

Having validated the transverse stress distribution given by (10), FE analyses were next employed to indirectly validate the critical far-field tensile stress associated with tension buckling given by (20). Two measures were taken to obtain the first buckling mode stress due to the transverse compressive stresses adjacent to the crack. First, only the web plates of PG-1 through PG-4 were modeled. Second, the out-of-plane translation of the web plate besides that of the embedded plate was restrained. 4-node shell elements were used to model the trial girder web plates. Each web plate was assigned the support conditions outlined in Table I. The clamped edge along the positive y-axis adjacent to the edge-crack was loaded with a unit transverse compressive stress distribution in the form given by (14). The first buckling mode stress was then computed for each web plate and the

Open Science Index, Civil and Environmental Engineering Vol:7, No:2, 2013 publications.waset.org/15693/pdf

corresponding far-field tensile stress was calculated from (14). The resulting critical far-field tensile stresses obtained from (20) and the FE analyses are summarized in Table III. The critical stress given by (20) is mostly conservative and is more accurate for longer crack lengths.

TABLE III
ANALYTICAL AND NUMERICAL TENSION BUCKLING STRESSES

Plate Girder (PG)	Eq. (20) (GPa)	FE Analysis (GPa)	% Error	Plate Girder (PG)	Eq. (20) (GPa)	FE Analysis (GPa)	% Error
PG-1a	4.77	5.83	18.2	PG-3a	76.4	67.2	-13.7
PG-1b	1.23	1.57	21.7	PG-3b	19.7	22.0	10.5
PG-1c	0.33	0.43	23.3	PG-3c	5.28	6.61	20.1
PG-1d	0.10	0.10	0.00	PG-3d	1.55	1.52	-1.97
PG-2a	19.1	21.2	9.91	PG-4a	305	156	-95.5
PG-2b	4.93	6.04	18.4	PG-4b	79.0	69.6	-13.5
PG-2c	1.32	1.72	23.3	PG-4c	21.2	24.1	12.4
PG-2d	0.39	0.39	0.00	PG-4d	6.18	5.85	-5.64

V. RESULTS AND DISCUSSION

The bending moment capacities of the trial girder web plates given by (21) were plotted as functions of edge-crack length (see Fig. 9). The horizontal portions of the plots indicate the elastic bending moment capacities. The web plate capacities of PG-1 and PG-2 were controlled by tension buckling when the crack lengths were 7 cm and 14 cm, respectively. The web plate capacities of PG-3 and PG-4 remained unaffected by tension buckling for all crack lengths.

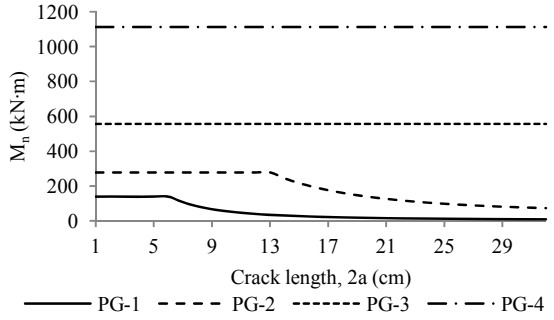


Fig. 9 Bending moment capacities of PG-1 through PG-4 web plates plotted as functions of crack length

Alternative failure modes of the trial girders including flange local buckling, lateral-torsional buckling, elasto-plastic failure, and brittle fracture were not considered in this study. Tension buckling is concluded to be an unlikely mode of failure in web-cracked girders unless the web is exceptionally thin or the crack is very large in comparison to the web depth. The expressions given by (20) and (21) could be used by engineers as an additional design check for the bending moment capacity of an I-shaped beam or plate girder considering existing or presumed vertical web-crack configurations.

REFERENCES

[1] Kouba, N.G., and Stallmeyer, J.E., "The behavior of stiffened beams under repeated loads," University of Illinois, Urbana, IL, Struct. Research Series No. 173, 1959.
[2] Yen, B.T., "On the fatigue strength of welded plate girders," Lehigh University, Bethlehem, PA, Fritz Eng. Lab. Rep. No. 303-1, 1963.
[3] Hall, L.R., and Stallmeyer, J.E., "Thin web girder fatigue behavior as influenced by boundary rigidity," University of Illinois, Urbana, IL, Structural Research Series No. 278, 1964.
[4] Goodpasture, D.W., and Stallmeyer, J.E., "Fatigue behavior of welded thin web girders as influenced by web distortion and boundary rigidity," University of Illinois, Urbana, IL, Structural Research Series No. 328, 1967.
[5] Yen, B.T., and Mueller, J.A., "Fatigue tests of large-size welded plate girders," Lehigh University, Bethlehem, PA, Fritz Eng. Lab. Rep. No. 303-10, 1966.
[6] Mueller, J.A., and Yen, B.T., "Girder web boundary stresses and fatigue," Lehigh University, Bethlehem, PA, Fritz Eng. Lab. Rep. No. 327-2, 1967.
[7] Marek, P., Perlman, M., Pense, A.W., and Tall, L., "Fatigue tests on a welded beam with pre-existing cracks," Lehigh University, Bethlehem, PA, Fritz Eng. Lab. Rep. No. 358-4A, 1970.
[8] Davies, A.W., Roberts, T.M., Evans, H.R., and Bennett, R.J.H., "Fatigue of slender web plates subjected to combined membrane and secondary bending stresses," J. Construct. Steel Research, vol. 30, no. 1, pp. 85-101, 1994.
[9] Roberts, T.M., Davies, A.W., and Bennett, R.J.H., "Fatigue shear strength of slender web plates," J. Struct. Eng., vol. 121, no. 10, pp. 1396-1401, 1995.
[10] Crocetti, R., "Web breathing of full-scale slender I-girders subjected to combined action of bending and shear," J. Construct. Steel Research, vol. 59, no. 3, pp. 271-290, 2003.
[11] Meguid, S.A., Engineering Fracture Mechanics. New York, NY: Elsevier Science Publishing Co., Inc., 1989, secs. 1.17, 4.3, 5.4, 6.1.
[12] Lawn, B., Fracture of Brittle Solids, 2nd ed. E.A. Davis, and I.M. Ward, Eds. Cambridge, UK: Cambridge University Press, ch. 9.
[13] Rolfe, S.T., and Barsom, J.M., Fracture and Fatigue Control in Structures: Applications of Fracture Mechanics. Englewood Cliffs, NJ: Prentice-Hall, 1977, ch. 7.
[14] Brighenti, R., "Buckling sensitivity analysis of cracked thin plates under membrane tension or compression loading," Nuclear Eng. and Design, vol. 239, no. 6, pp. 965-980, 2009.
[15] Roberts, R., Fisher, J.W., Irwin, G.R., Boyer, K.D., Hausammann, G.V., Krishna, V., Morf, R., and Slockbower, R.E., "Determination of tolerable flaw sizes in full size welded bridge details," Lehigh University, Bethlehem, PA, Fritz Eng. Lab. Rep. No. 399-3, 1977.
[16] Roberts, T.M., Osman, M.H., Skaloud, M., and Zornerova, M., "Residual shear strength of fatigue cracked slender web panels," Thin-Walled Struct., vol. 24, no. 2, pp. 157-172, 1996.
[17] Narayanan, R., and Der-Avanessian, N., " Design of slender webs having rectangular holes," J. Struct. Eng., vol. 111, no. 4, pp. 777-787, 1985.
[18] Cooper, P.B., and Roychowdhury, J., "Shear strength of plate girders with web openings," J. Struct. Eng., vol. 116, no. 7, pp. 2042-2048, 1990.
[19] Ito, M., Fujiwara, K., and Okazaki, K., " Ultimate strength of beams with U-shaped holes in top of web," J. Struct. Eng., vol. 117, no. 7, pp. 1929-1945, 1991.
[20] Zaarour, W., and Redwood, R., "Web buckling in thin webbed castellated beams," J. Struct. Eng., vol. 122, no. 8, pp. 860-866, 1996.
[21] Bedair, O., "Stress analyses of deep plate girders used at oil and gas facilities with rectangular web penetrations," Practice Periodical on Struct. Design and Construct., vol. 16, no. 3, pp. 112-120, 2011.
[22] Guz, A.N., and Dyshel, M.Sh., "Fracture and buckling of thin panels with edge crack in tension," Theo. and Appl. Fract. Mech., vol. 36, no. 1, pp. 57-60, 2001.
[23] Guz, A.N., and Dyshel, M.Sh., "Stability and residual strength of panels with straight and curved cracks. Theo. and Appl. Fract. Mech., vol. 31, nos. 1-3, pp. 95-101, 2004.
[24] Vafai, A., and Estekanchi, H.E., "A parametric finite element study of cracked plates and shells," Thin-Walled Struct., vol. 33, no. 3, pp. 211-229, 1999.
[25] Brighenti, R., "Buckling of cracked thin-plates under tension or compression," Thin-Walled Struct., vol. 43, no. 2, pp. 209-224, 2005.

Open Science Index, Civil and Environmental Engineering Vol:7, No:2, 2013 publications.waset.org/15693/pdf

[26] Brighenti, R., "Numerical buckling analysis of compressed or tension cracked thin plates," Eng. Struct., vol. 27, no. 2, pp. 265-276, 2005.
[27] Shimizu, S., "Tension buckling of plate having a hole," Thin-Walled Struct., vol. 45, nos. 10-11, pp. 827-833, 2007.
[28] Brighenti, R., "Buckling sensitivity analysis of cracked thin plates under membrane tension or compression loading," Nuclear Eng. and Design, vol. 239, no. 6, pp. 965-980, 2009.
[29] Kumar, Y.V.S., and Paik, J.K., "Buckling analysis of cracked plates using hierarchical trigonometric functions," Thin-Walled Struct., vol. 42, no. 5, pp. 687-700, 2004.
[30] Sun, C.T., and Jin, Z.-H., Fracture Mechanics. Waltham, MA: Academic Press, 2012, sec. 3.5.
[31] Sadd, M.H., Elasticity: Theory, Applications, and Numerics, 2nd ed. Burlington, MA: Academic Press, 2009, secs. 5.5, 7.5.
[32] Westergaard, H.M., "Bearing pressures and cracks," J. Applied Mech., vol. 6, no. 61, pp. 49-53, 1939.
[33] Sedov, L.I., A Course In Continuum Mechanics. J.R.M. Radok, Trans. Groningen, Netherlands: Wolters-Noordhoff Publishing, 1972, sec. 13.2.8.
[34] Fett, T. Stress Intensity Factors, T-Stresses, Weight Functions. Karlsruhe, Germany: Universitätsverlag Karlsruhe, 2008.
[35] Vinson, J.R., Structural Mechanics: The Behavior of Plates and Shells. New York, NY: John Wiley & Sons, Inc., 1974, sec. 6.1.

Open Science Index, Civil and Environmental Engineering Vol:7, No:2, 2013 publications.waset.org/15693/pdf